CASL-U-2012-0171-000

Power uprates
and plant life extension

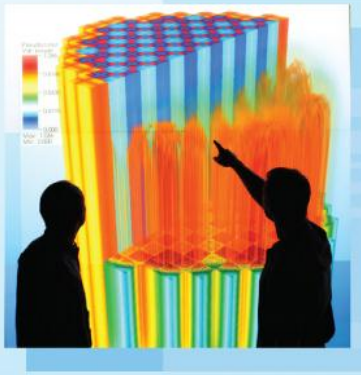

Engineering design
and analysis

Science-enabling
high performance
computing

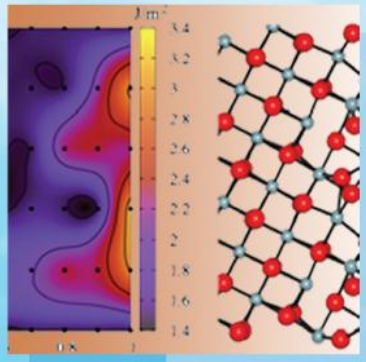

Fundamental science

Plant operational data

Consortium for Advanced Simulation of LWRs

L3:THM.CFD.P5.04

Mark Christon
LANL

Completed: 11/26/2012

U.S. DEPARTMENT OF ENERGY | Nuclear Energy

Grid Sensitivity Study of CFD versus COBRA

L3:THM.CFD.P5.04 Milestone Report

Dr. J. Michael Doster and Murray Thames
Department of Nuclear Engineering
North Carolina State University

November, 2012

1. Introduction:

The Industry Standard for clad temperature prediction and critical heat flux calculations (subchannel analysis) relies on a finite difference approach to evaluate thermal conditions in core flow channels at specified axial locations. This provides a pseudo three-dimensional capability, allowing for the channel-averaged fluid and clad temperature to be modeled throughout the entirety of the core. This approach allows for quick prediction of both transient and steady-state scenarios with reasonably accurate results. However, this limited 3D capability and averaged equation formulation may not allow for the representation of true peak clad temperatures. With current computing capabilities, a full three-dimensional navier-stokes approach may be possible. This may provide a higher level of accuracy, while also allowing for the thermal-hydraulic conditions to be known at any location throughout the core.

CFX is a finite element based computational fluid dynamics code that utilizes the navier-stokes equations to evaluate complex fluid systems. This program uses meshes produced from the ANSYS mesh generation tool. The tool itself automatically generates a mesh, but allows for some limited customization to the mesh properties. Once the mesh is obtained, the solver employs a high resolution scheme which minimizes the root-mean square residuals to some user defined convergence criteria. Under turbulent flow conditions, the user is able to select a turbulent closure model which is employed in the three-dimensional navier stokes equations. For the cases examined here, both the k-epsilon model and Speziale, Sarkar and Gatski (SSG) Reynolds Stress model were used.

This particular study focuses on a comparison between the subchannel code COBRA and the CFX computational fluid dynamics package at various mesh sizes. A set of initial and boundary conditions were obtained from the COBRA test case CBRSPC1, and were then modified to prevent wall temperatures from exceeding the saturation temperature. The parameters for this case can be found in Table 1-1.

Table 1-1: 17x17 Assembly Parameters

Vertical Length (in):	167.992
Number of Fuel Rods:	265
Number of Water Rods:	25
Mass Flux (lbm/hr-ft^2):	2.54E+06
Inlet Enthalpy (Btu/lbm):	559
Rod Diameter (in):	0.374
Pitch (in):	0.4704
Pressure (psia):	2163
Flow Area (ft^2):	0.0349

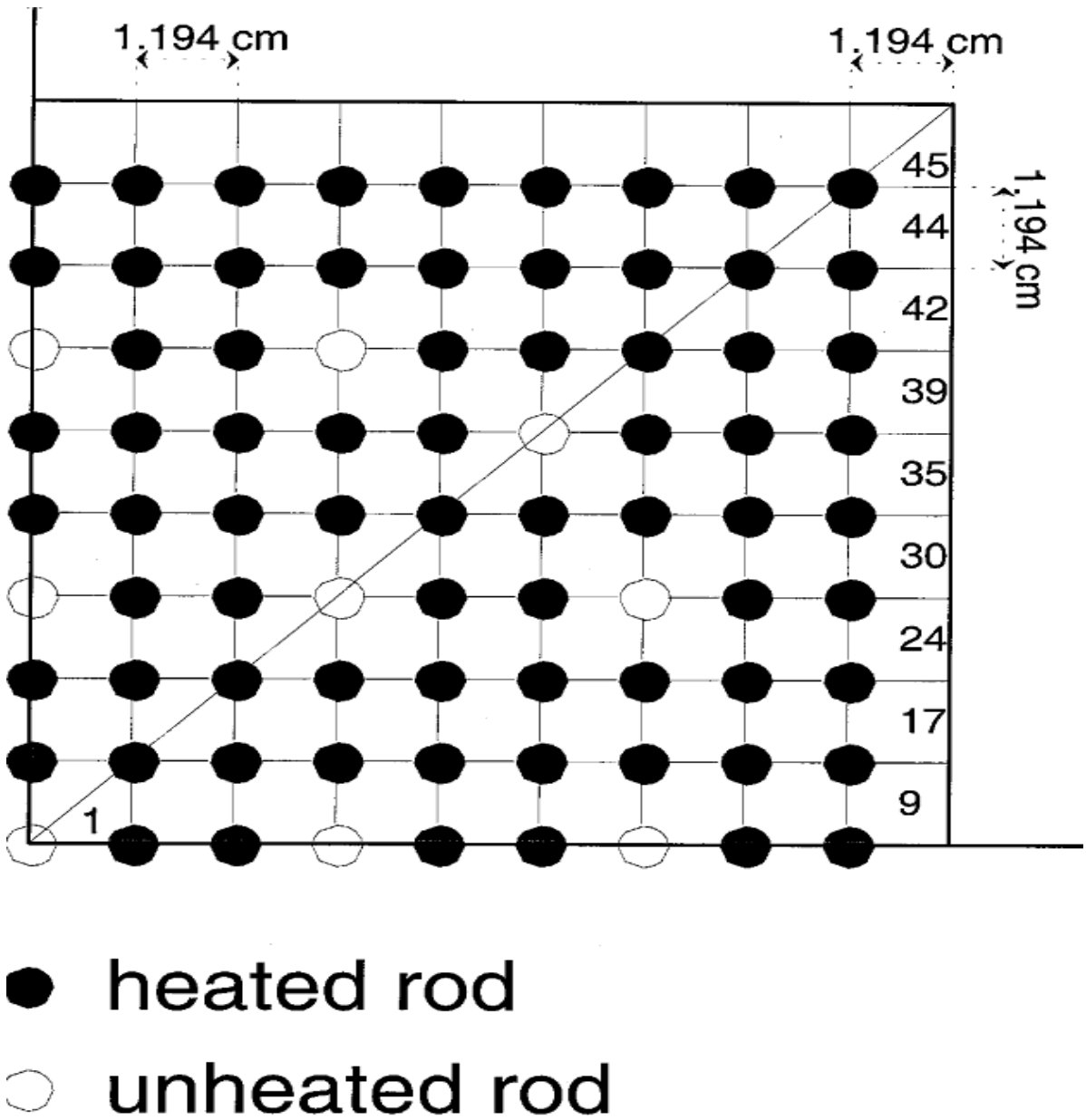

Figure 1-1: Upper-Right Quadrant of the 17x17 Assembly

								0.8801
							0.9524	0.9133
						0.9898	0.9646	0.9193
					0	1.0155	0.9795	0.9278
				1.0469	1.0487	1.0337	0.9972	0.9372
			0	1.0437	1.0415	0	1.0085	0.9436
		1.0299	1.0386	1.0305	1.0275	1.0267	1.003	0.9446
	1.0306	1.0301	1.0376	1.0291	1.0258	1.0253	1.0032	0.946
0	1.0428	1.0435	0	1.042	1.0382	0	1.0135	0.9482

Figure 1-2: Power Profile for Lower Half of Upper-Right Quadrant

All linear heat rates obtained from COBRA were converted to surface heat fluxes for each rod. These heat fluxes were fit to a set of 45 sixth-degree polynomials and then input into CFX. Of interest is the wall temperature distribution in the hottest rod (Rod 32) as well as the convective heat transfer coefficient for that rod. The problem parameters and peaking factors can be found in Table 1-1, Figures 1-1 and 1-2.

Studies have been performed by other researchers that compare CFD predictions in rod bundles to experimental data. The experimental apparatus for each study was designed to approximate the thermal-hydraulic conditions in a typical PWR assembly, but were scaled down for ease of development. The parameters of interest ranged from azimuthally measured convective heat transfer coefficients near grid spacers and mixing vanes to axial pressure drops along the bundle. While these parameters were not the focus of this study, these findings help to draw conclusions regarding the relative merits of CFD versus traditional sub-channel methods for PWR applications. Of particular interest were the mesh and turbulence models utilized in other CFD studies compared to the optimal ones found in this study.

2. Literature Review:

Great strides have been made to develop CFD codes that can be applied to Reactor geometries and conditions. Currently CFD is used in Westinghouse's thermal-hydraulic design to predict flow properties downstream of a spacer grid. Their CFD methodology involves the use of CD-ADAPCO's CFD code: STAR-CD [1]. This software's pre-processing may be used to generate a variety of structured or un-structured meshes. This software has been utilized in other case studies which validate the use of CFD in the thermal-hydraulic evaluation of reactor fuel bundles. The specific parameters of interest in the thermal-hydraulic evaluation studies are wall heat transfer coefficients, peak wall temperatures, lateral cross flow and pressure drops across grid spacers. These quantities strongly determine the onset of DNB in single-phase dominated systems.

Conner et Al. directly cites the use of Westinghouse methodology in development of their CFD study [1]. Their study focused on observing circumferential heat transfer coefficients downstream of a mixing device within a 5x5 test assembly. The test assembly consisted of 5 rods which were uniformly heated both axially and azimuthally. This study utilized air flowing at 5 m/s as the test fluid. A similar study was performed which evaluated the circumferential temperature profile within a 37-rod test assembly [2]. The rods were uniformly heated, with an estimated surface heat flux of 1.37 W/m^2. The bulk velocity of air flowing through the assembly was 22.7 m/s, which produced a Reynolds number of 66,500. This experimental set-up was then used by Baglietto as a benchmark to evaluate the effects of a non-linear, anisotropic k-epsilon model [3].

Other cases examined did not directly deal with wall parameters, but rather local flow conditions. Ikeda and Hoshi [4] evaluated the effect of cross flow on peak fluid temperatures within a 5x5 and a 3x3 test assembly. Both assemblies contained spacer grids, but the 3x3 assembly contained mixing vanes within the grid. The 5x5 assembly was used to compare pressure drop values obtained from STAR-CD to the measured value. Due to the presence of mixing vanes within the 3x3 assembly, it was an ideal candidate for coolant mixing (cross flow). Ikeda et Al. [5] also performed a study which focused more specifically on pressure drop calculations across a spacer grid. This study utilized a similar 5x5 experimental set-up, with 3 spacer grids located uniformly along the length of the assembly. The conditions used in this case were more identical to reactor conditions with Reynolds numbers up to 500,000, fluid temperatures of 150 °C, and a system pressure of 0.6 MPa.

All studies utilized similar approaches to meshing and turbulence modeling within STAR-CD. Due to the complexity of the flow within fuel bundles, a fine mesh approach was typically chosen. Conner et Al. [1] utilized a cubic hexahedra based mesh within their 5x5 test assembly. This type of mesh was chosen over tetrahedral due to issues that can arise when refinement is needed in tetrahedron based meshes (grid quality, aspect ratio and skewness). To accurately predict the turbulence generated from fluid-to-wall shear, the mesh was inflated near the rod surfaces. The final mesh size used for computation consisted of 20 million elements. Baglietto [3] used a base mesh which contained 50,000 cells per axial plane. Mesh coarsening was applied to validate the turbulence model at coarser grids. This reduced the cells per axial plane to 7000, 3700 and 1280 for each case. Ikeda and Hoshi [4] generated a grid which contained 2 million total fluid elements for validation of pressure drop calculations in their 5x5 assembly. In the final 5x5 case study performed by Ikeda et Al. [5], the mesh generated was composed of hexahedra, tetrahedral and triangular prisms. This unstructured mesh allowed for

accurate representation of the grid spacer geometry used in this study. This mesh contained approximately 7 million elements.

Turbulence modeling is a crucial part of accurate flow prediction within the test assemblies. For all cases, the k-epsilon model was utilized for turbulence closure. However, each study used slightly different variations of k-epsilon to predict turbulence. The Renormalization (RNG) k-epsilon model was chosen in the study by Conner et Al. [1]. This model had the best agreement with experiment since it accurately modeled the effects of curvature and rotation in the turbulence dissipation rate equation. Baglietto [3] examined the effect of a newly formed non-linear, anisotropic turbulence model. This model is seen as advantageous in the vicinity of spacer grids, since turbulence is not considered isotropic in this region. Ikeda et al. [5] chose to compare the effects of two different turbulence models: the standard k-epsilon and a non-linear, anisotropic model (similar to that considered by Baglietto). Also considered was utilizing a Reynolds Stress model, but the computational cost would have increased significantly.

The results provided from the CFD analysis provide an optimistic outlook for this type of methodology. The circumferential heat transfer profile produced from STAR-CD was similar to that obtained from experimental measurements [1]. The fluid that was used in the CFD analysis itself was water, while the experiment was conducted with air. This led to magnitude differences in the heat transfer coefficients, but the locations where heat transfer either spiked or dropped were identical in both the CFD results and experimental results. Baglietto [3] found that the circumferential wall temperature profiles differed slightly from the experimental results. This led to the identification of an issue with the constant heat flux assumption. After adjusting the set-up to also solve the conjugate heat transfer problem produced by the rods, the CFD results agreed with the experimental measurements.

The results obtained by Ikeda and Hoshi [4] were used to characterize the DNB performance of a given grid geometry. Geometries that yielded a lower peak fluid temperature were said to have better DNB performance. The grids that contained the most mixing vanes would then produce lower peak fluid temperatures due to increased coolant mixing. CFD analysis found that the grid that contained 18 mixing vanes resulted in a lower peak fluid temperature relative to a grid that contained 12 vanes. Additional CFD tests were performed which involved gradually shifting the geometry in order to reduce the peak fluid temperature. This essentially outlined using CFD as a tool for the design of effective spacer grids. Ikeda et al. [5] found that pressure drops calculated using both turbulence models were very close to the measured value. However, the standard k-epsilon model performed poorly in evaluating the pressure drop directly across a spacer grid. This led to over predicting the pressure drop by up to 11%. The anisotropic model produced values within 5% of that expected for this particular case. In addition, the standard k-epsilon model was found to under predict the values of turbulent kinetic energy downstream of the spacer grid. It was concluded that this issue arose from the isotropic assumption inherent in the standard k-epsilon model.

3. Mesh Selection:

In previous reports we documented the performance degradation with increasing mesh size of CFD versus Subchannel calculations of wall temperature for PWR rod bundles. A summary of those results is presented below. The original mesh chosen for CFD to COBRA comparisons was tetrahedral, developed using ANSYS' mesh generation package. The finest and

coarsest tetrahedral mesh cases are labeled in figures 3-1 and 3-2. At the finest scale, inflation layers (refinement) were added near the rod surfaces and near the assembly wall (not shown). To understand the restrictions that mesh size imposed on the solution, the coarse mesh case removed all inflation layers and increased the average element size.

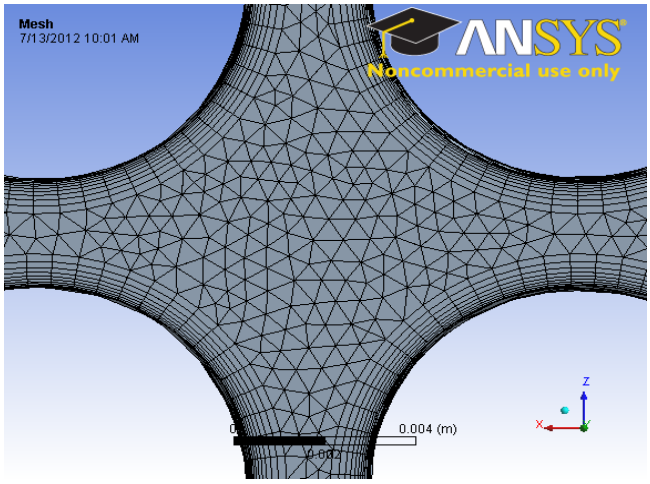

Figure 3-1: Fine Tetrahedral Mesh (68e6 elements)

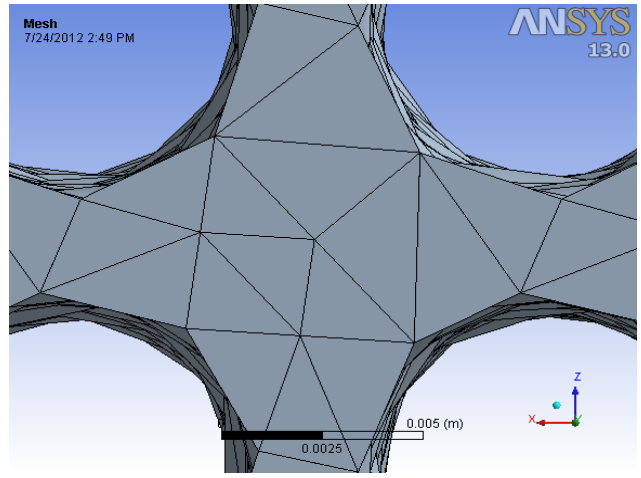

Figure 3-2: Coarse Tetrahedral Mesh (2.4e6 elements)

Further studies were performed to evaluate the effect of other mesh types on the solution. The second mesh type was formed by cubic hexahedral cells. ANSYS mesh generation restricted the use of inflation with this setting, so the finest resolution consisted of 18 million elements (show in Figure 3-3). The mesh was then gradually coarsened until the 0.4 million element mesh shown in Figure 3-4 was obtained. The mesh was able to be coarsened to such a low element number due to relatively small changes in the computed wall temperature solution with large decreases in mesh resolution.

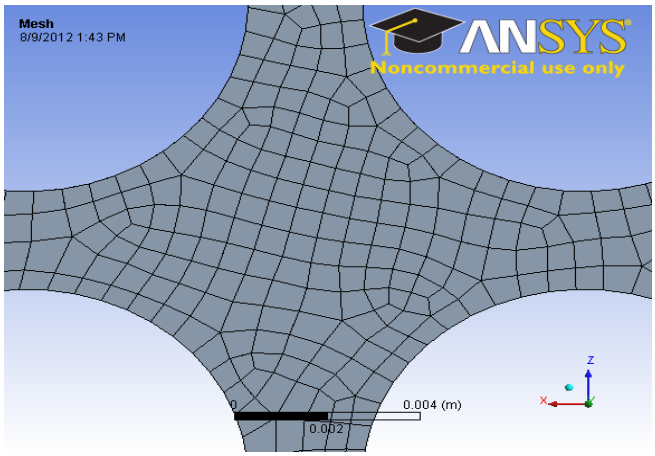

Figure 3-3: Fine Hexahedral Mesh (18e6 elements)

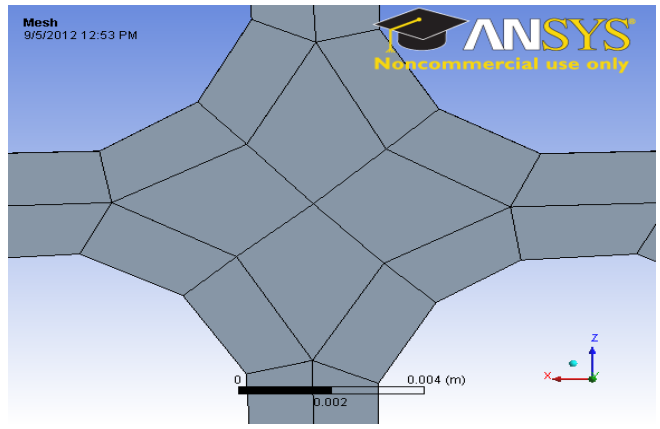

Figure 3-4: Coarse Hexahedral Mesh (0.4e6 elements)

4. Results and Discussion:

Figures 4-1 through 4-4 contain the results obtained for a specified mesh size and the two different turbulence models considered. COBRA results are also displayed. The results presented are for the hottest rod within the assembly (Rod 32). For every selection of mesh and turbulence model, one parameter of interest (heat transfer coefficient or wall temperature) may agree with the COBRA results, but there was not a case where both parameters agreed. Since CFX-Post does not yield wall temperatures directly, the wall temperature was calculated according to equation 4.1:

$$T_w = \frac{q''}{h_c} + T_{nw} \qquad (4.1)$$

where q'' is the wall heat flux, h_c is the wall heat transfer coefficient and T_{nw} is the temperature at the internal near-wall boundary center node. Since the version of COBRA utilized in this work solves only a one-dimensional conduction equation at any axial location, only average values from the CFD calculations are presented for comparison. As documented in previous reports, even for uniform circumferential heat fluxes, the CFD results predict significant variations in the wall temperatures at any axial location, highlighting the weakness in the one-dimension treatment in the subchannel calculations.

Figure 4-1 shows the relative difference of heat transfer coefficient values obtained when utilizing either the k-epsilon model or SSG model. The SSG model produced values that were much closer to those obtained through COBRA. This is most likely due to the accurate predictions of turbulence in the SSG model, which directly affects the heat transfer capability from the rod surface to the liquid. However, it is interesting to note that the k-epsilon model was found to under predict the turbulent kinetic energy by Ikeda et al [5]. This would lead to lower values of heat transfer, rather than the higher values that can be observed.

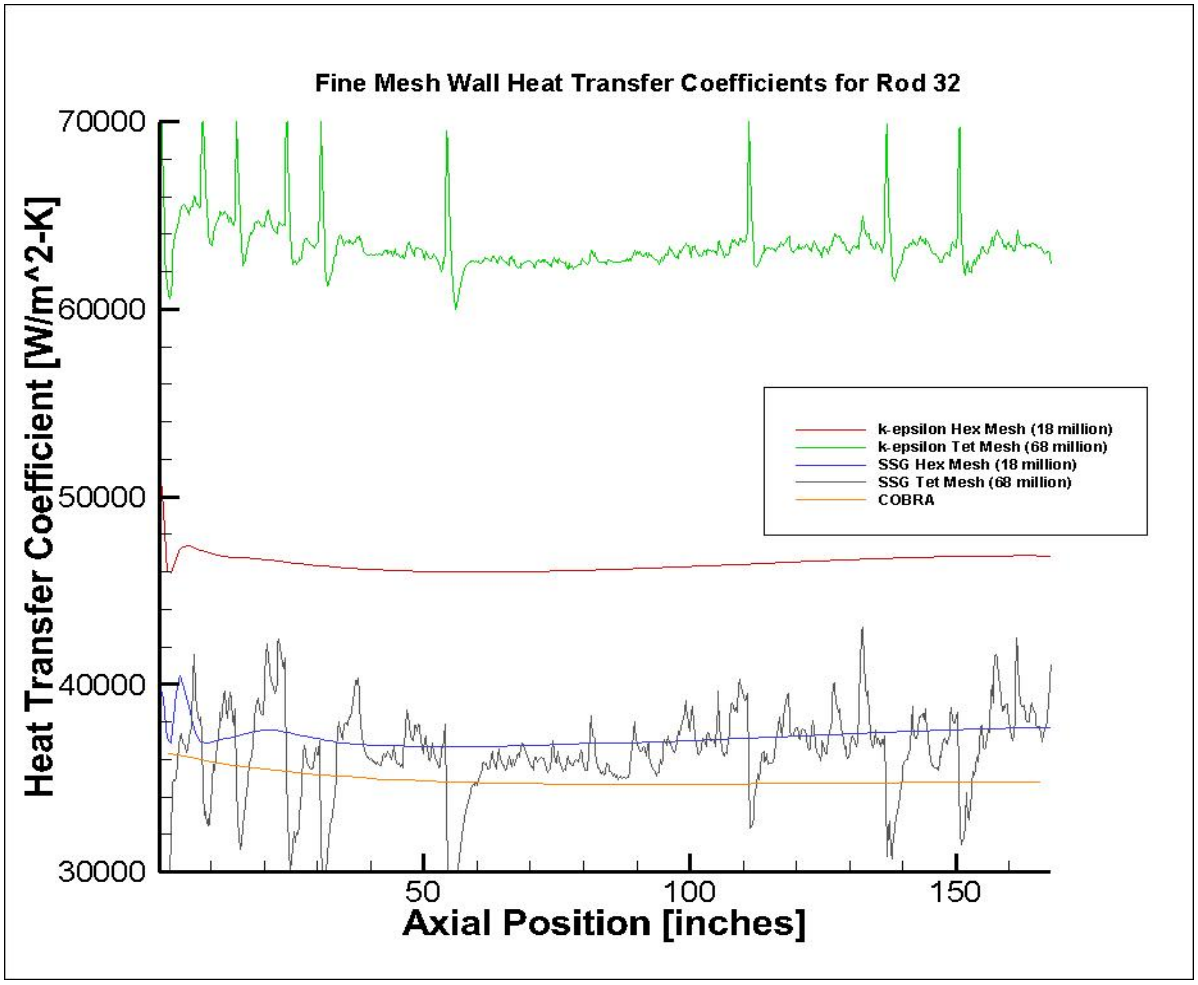

Figure 4-1: Fine Mesh Wall Heat Transfer Coefficients

In addition, differences are clear between the two mesh selections. The tetrahedral mesh produces negative and positive spikes at various axial locations. It can be observed that where a negative spike occurs in the SSG results, a positive spike occurs at the exact same location for the k-epsilon model. These anomalies are not present in the cubic hex mesh for either turbulence model. The spikes that occur with the tetrahedral based mesh could have arisen due to the issues stated by Conner et al. [1]. In particular, highly skewed tetrahedrons may have led to the development of rapid changes in the solution, thus producing this spiked behavior.

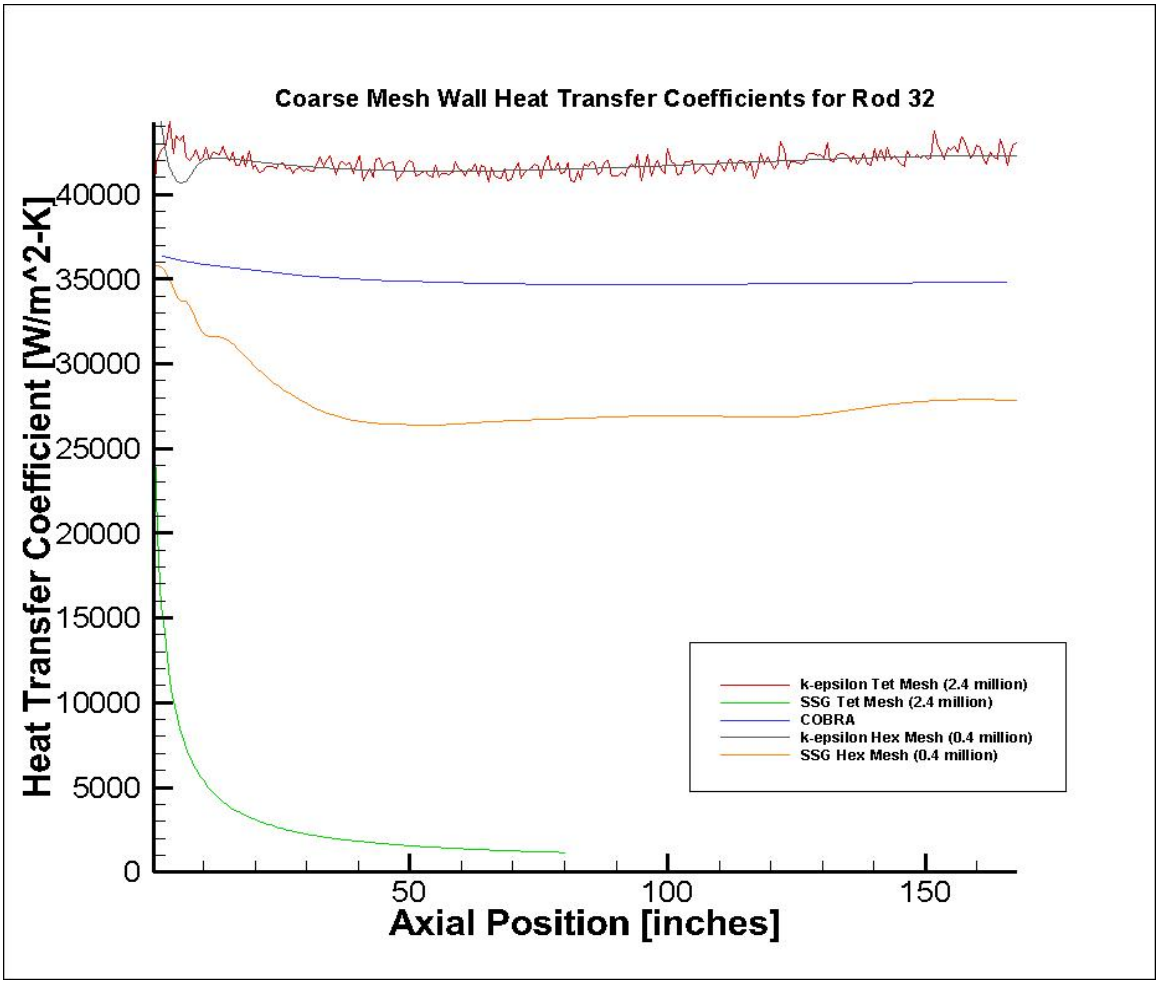

Figure 4-2: Coarse Mesh Wall Heat Transfer Coefficients

The heat transfer coefficient results for coarse mesh runs are specified in Figure 4-2. The changes that occur with each turbulence model tended to follow a similar trend: as the mesh is coarsened, the resulting heat transfer coefficient decreases. This behavior was much more noticeable for the tetrahedron meshes, particularly the SSG model. This issue became so severe for the SSG model that the average heat transfer coefficient was an order of magnitude less for the coarsest mesh. However, this decrease in the heat transfer coefficient brought the k-epsilon model's result more in line with that obtained from COBRA.

The effect of mesh coarsening on the heat transfer coefficient solution is due to inaccurate turbulence results. As the mesh is coarsened, eddy production due to fluid shear from the wall is not fully captured. This leads to lower values of turbulent kinetic energy, which relates to adequate coolant mixing and convective heat transfer. In addition, the heat input may not be accurately approximated since there are a reduced number of elements lining the surface of the rods.

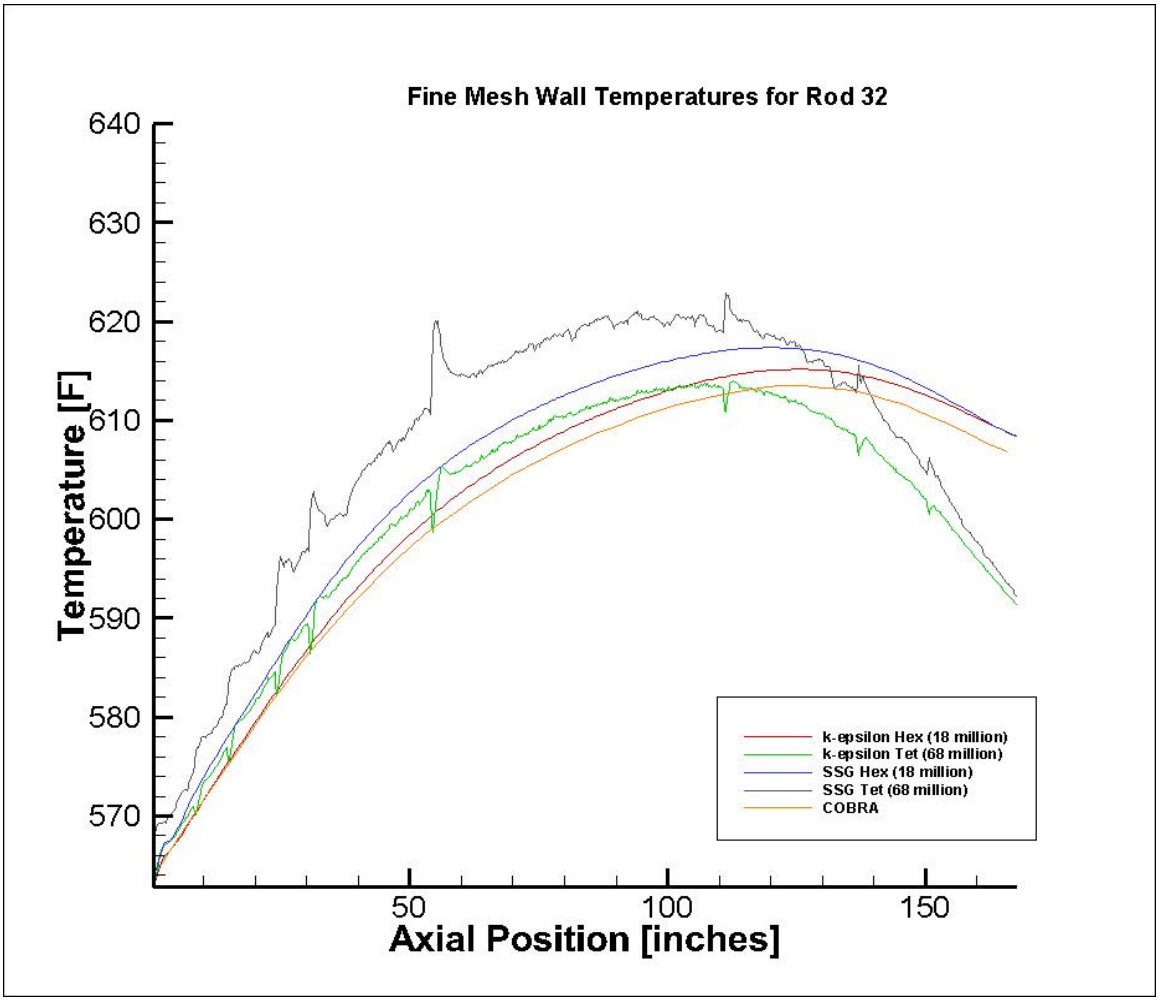

Figure 4-3: Fine Mesh Wall Temperature

The wall temperatures found in Figure 4-3 are directly related to the heat transfer coefficients found in Figure 4-1. The tetrahedron mesh produced wall temperatures that spiked at locations where the heat transfer dropped, with the opposite occurring for spikes in heat transfer. This leads to the tetrahedron temperature profiles having a similar erratic behavior as that found in the heat transfer coefficient profile. As would be expected, the greatest difference in the CFD and COBRA results occur in regions of highest wall heat flux, i.e. midway along the channel.

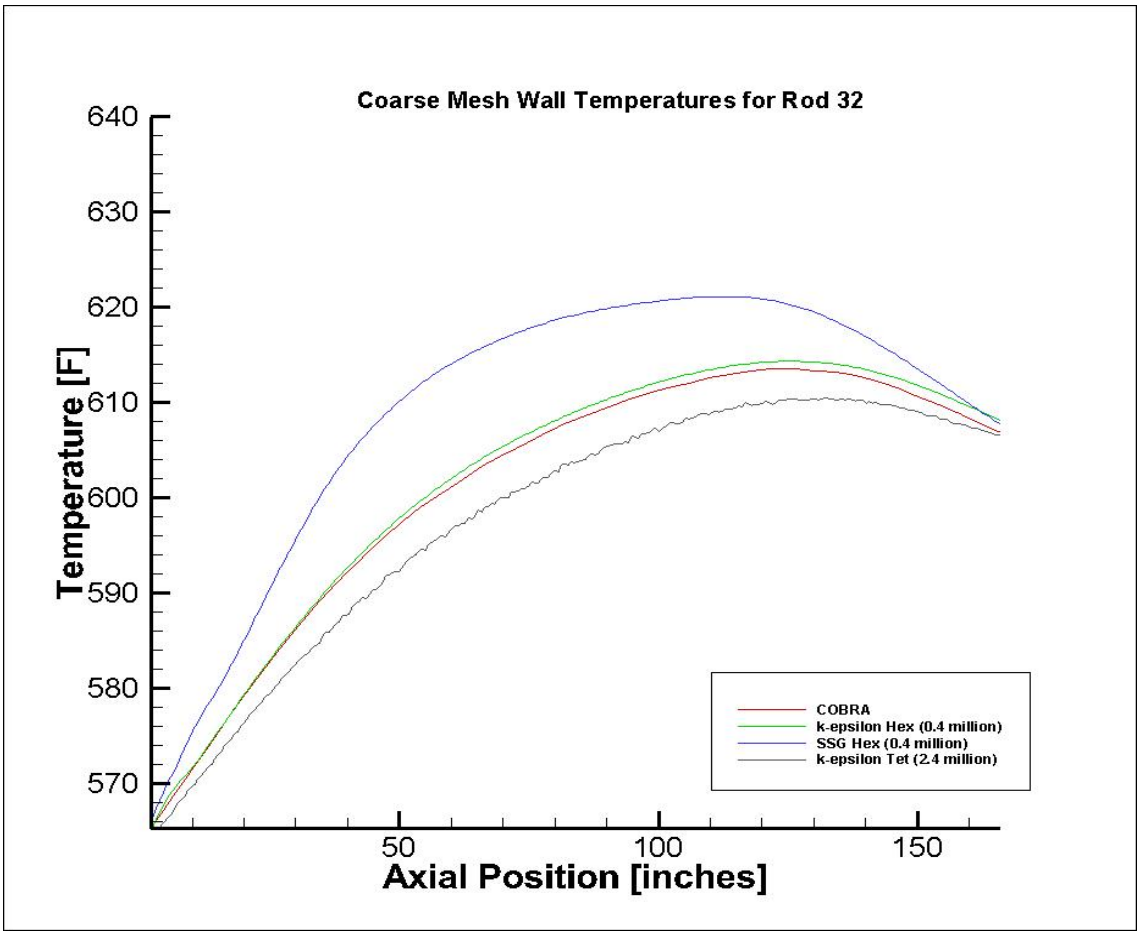

Figure 4-4: Coarse Mesh Wall Temperature

The coarse mesh wall temperature results (Figure 4-4) produce the profile that is nearest the COBRA profile. The k-epsilon model applied to the hexahedron mesh yielded a temperature profile that is almost identical (in the lower region of the channel) to that obtained from COBRA. The SSG model is shown to perform very poorly for this mesh type due to extremely large wall temperature predictions midway up the channel.

The tetrahedral mesh produced smoother results for the k-epsilon model at this mesh resolution compared to the finest resolution. This is due to smaller variations in the heat transfer coefficient for this case. Since the heat transfer coefficient for the SSG model dips so low, the resulting wall temperature was too high to be displayed in Figure 4-4.

5. Conclusion:

CFD can be a powerful tool for the evaluation of reactor thermal-hydraulic properties. This is evident from the benchmarking studies referenced. It is still not clear whether CFD is superior to Subchannel methods in areas far from spacer grids. CFD requires very extensive geometry definition in order to be successful. In addition, it was seen that mesh generation plays a huge role in the accuracy of the solution obtained through CFD. This particular aspect can lead

to issues due to restrictions in computational power. If Subchannel methods are used, problem definition can be relatively quick, while still retaining a high level of accuracy. However, choosing Subchannel methods restricts the dimensionality of the solution and detailed information in the vicinity of spacer grids is lost, as well as circumferential variations in wall temperature unless more detailed heat conduction models are employed in the subchannel solution. Additional benchmarking studies, which specifically compare the results obtained by both Subchannel methods and CFD, are required to further assess this problem. In particular, comparisons which explicitly include variations in the heat generation rate within fuel rods, and conjugate heat transfer will be required to fully assess the relative differences in the methods.

References:

[1] M. E. Conner, E. Baglietto and A. M. Elmahdi. 2010. "CFD methodology and validation for single-phase flow in PWR fuel assemblies." *Nuclear Engineering and Desig*, Vol. 240, No. 9, pp. 2088-2095.

[2] L. Meyer. 1994. "Measurements of turbulent velocity and temperature in axial flow through a heated rod bundle." *Nuclear Engineering and Design*, Vol. 146, pp.71-82.

[3] E. Baglietto. 2006. "Anisotropic Turbulence Modeling for Accurate Rod Bundle Simulations." Proceedings of 14th International Conference on Nuclear Engineering, Miami, Florida, USA, July 17-20, Paper No. ICONE14-89646.

[4] K. Ikeda and M. Hoshi. 2002. "Development of Mitsubishi High Thermal Performance Grid." *JSME International Journal*, Vol. 45, No. 3, pp. 586-591.

[5] K. Ikeda, J. Shimizu, Y. Yamaguchi, and K. Okamoto. 2009. "Study of Spacer Grid Span Pressure Loss under High Reynolds Number Flow Condition." Proceedings of 17th International Conference on Nuclear Engineering, Brussels, Belgium, July 12-16, Paper No. ICONE17-75925.